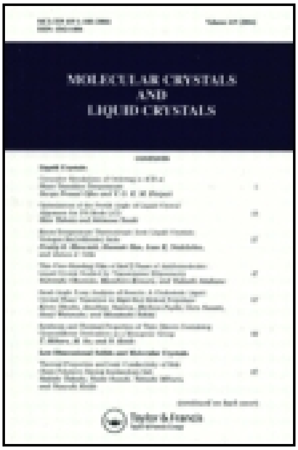

Molecular Crystals and Liquid Crystals

Publication details, including instructions for authors and subscription information:
http://www.tandfonline.com/loi/gmcl16

Scaled Particle Theory of a System of Hard Right Circular Cylinders

K. L. Savithramma [a] & N. V. Madhusudana [a]

[a] Raman Research Institute, Banglore, 560080, India

Version of record first published: 14 Oct 2011.

To cite this article: K. L. Savithramma & N. V. Madhusudana (1981): Scaled Particle Theory of a System of Hard Right Circular Cylinders, Molecular Crystals and Liquid Crystals, 74:1, 243-259

To link to this article: http://dx.doi.org/10.1080/00268948108073709

Mol. Cryst. Liq. Cryst., 1981, Vol. 74, pp. 243-259
0026-8941/81/7404-0243 $06.50/0

Printed in the United States of America

Scaled Particle Theory of a System of Hard Right Circular Cylinders†

K. L. SAVITHRAMMA and N. V. MADHUSUDANA
Raman Research Institute, Bangalore 560080, India

(*Received August 18, 1980; in final form February 10, 1981*)

We have applied the scaled particle theory to a system of hard right circular cylinders. By varying the radius to height ratio R, we can study either rod-like molecules ($R < 0.5$) or disc-like molecules ($R > 0.5$). We have calculated the packing fraction d_{nem}, the density jump ($\Delta\rho/\bar{\rho}$), the order parameters $<P_{2n}>$, the entropy change $\Delta S/Nk$, Pv_0/kT and the isothermal compressibility β of the isotropic phase at the nematic-isotropic transition point for a range of values of R. By expanding the angle dependent terms occurring in the theory in a series of even Legendre polynomials, it is found that terms at least up to $P_4(\cos\theta)$ have to be retained to get qualitatively correct results. The thermodynamic properties at the nematic-isotropic transition point appear somewhat symmetrical for the rod-like and disc-like regions if they are plotted as functions of the ratio (largest dimension/shortest dimension) of the cylinders.

INTRODUCTION

The importance of the geometrical features of the molecules in determining the properties of nematic liquid crystals has been recognized for a long time. In fact there have been several attempts (see for example, Refs. 1-4) to describe the nematic phase in terms of hard-rod models. The most successful attempts[5-8] to quantitatively describe the properties of the nematic phase have included both the hard-rod feature of the molecules as well as the attractive forces between them.

Disc-shaped molecules have been recently shown[9] to exhibit a new class of liquid crystalline phases (the discotic phases). Some of these have been found to exhibit a "fluid" phase with only a long range orientational order, i.e., a discotic nematic phase.[10] Indeed the nematic phase exhibited by essentially flat molecules was discovered long ago in the pyrolisis of coke.[11] The effect of

---

† Presented at the Eighth International Liquid Crystal Conference, Kyoto, July 1980.

plate-like molecules on the nematic phase transition was discussed theoretically by Alben.[12] Isihara[13] has considered phase transition in anisotropic colloidal solutions consisting of disc-like molecules, in an approach similar to that of Onsager.[1]

As we have discussed elsewhere,[8] the scaled particle theory as developed by Cotter[5] gives a good description of the nematic phase of rod-like molecules. In this paper, we extend the scaled particle theory to the discotic nematic phase. In discussing the thermodynamic properties of the nematic phase made of rod-like molecules, it is conventional to assume that the molecules have a spherocylindrical shape. In order to be able to compare the results on disc-like molecules with those on rod-like molecules, we extend the theory to a system of right circular cylinders. If r is the radius of the cylinder and l its height, the shape-factor $R = r/l$ is >0.5 for disc-like molecules and <0.5 for rod-like molecules. We will in the next section, summarize the scaled particle theory of Cotter[5] as extended to such a system. As our present interest is to compare the properties of systems of rod-like and disc-like particles, we confine the theory in this paper to hard particles. The results for various properties of the system for different values of R will be presented and discussed in the last section.

THE SCALED PARTICLE THEORY

In this section we will give only a brief summary of the theory. For detailed derivations and discussion of the merits and demerits of the theory, reference may be made to Cotter's paper.[5]

Consider a system of N cylindrical molecules in a volume V and at a temperature T. Let m be the number of discrete orientations allowed for the molecules, such that N_1 molecules have orientation Ω_1, N_2 have orientation Ω_2, etc. *Choosing* the set $\{N_1 N_2 \ldots N_m\}$ which maximizes the partition function, the maximum term of the ensemble partition function is given by[5]

$$Q_N(N_1 \ldots N_m, V, T) = (N_1! \ldots N_m!)^{-1} \int \cdots \int \prod_{i=1}^{N} d^3 r_i \prod_{i=1}^{N} d\Omega_i \times \exp[-U_N(r_1 \ldots r_N;\, \Omega_1 \ldots \Omega_N)/kT]$$

where $N = \sum_{j=1}^{m} N_j$ and U_N is the energy of the N-particle system. For a system of *hard* particles, the interaction energy between two molecules is infinity when they come into contact with each other and zero otherwise. Then the configurational chemical potential μ_i^* of the i^{th} species oriented in the direction Ω_i is given by[5]

$$\mu_i^* = kT \ln \rho_i + W_i(\alpha, \lambda); \quad \lambda = \alpha = 1 \tag{1}$$

where $\rho_i = N_i/V$ is the number density of molecules of i^{th} type and $W_i(\alpha, \lambda)$ is the work function defined as the reversible work of adding a scaled hard cylindrical molecule of radius αr and height λl, oriented in the direction Ω_i to the fluid of N cylindrical molecules of radius r and height l. For α and λ which are sufficiently small so that three molecules of the fluid cannot be simultaneously in contact with the scaled particle, it can be written,[5]

$$\exp[-W_i(\alpha,\lambda)/kT] = 1 - \rho \sum_{j=1}^{m} S_j v_{ij} \tag{2}$$

where $S_j = N_j/N$ and $\rho = N/V$, v_{ij} is the volume excluded to the center of a regular cylinder with orientation j by the presence of the scaled cylinder and is given by[13]

$$\begin{aligned} v_{ij} &= \pi r^2 l(1 + \alpha^2\lambda) + \pi r^2 l(\alpha^2 + \lambda)\,|\cos\theta_{ij}| + 2\pi r^3(\alpha + \alpha^2)\sin\theta_{ij} \\ &\quad + 2rl^2(\alpha\lambda + \lambda)\sin\theta_{ij} + 4r^2 l(\alpha + \alpha\lambda)\int_0^{\pi/2}\sqrt{1 - \sin^2\theta_{ij}\sin^2\varphi}\,d\varphi \end{aligned} \tag{3}$$

For large values of α and λ, $W_i(\alpha,\lambda)$ must approach the reversible work of creating a macroscopic cylindrical cavity in the fluid, i.e.,

$$\lim_{\alpha\to\lambda\to\infty} W_i(\alpha,\lambda) = \pi\alpha^2\lambda r^2 l P^* = \alpha^2\lambda v_0 P^* \tag{4}$$

where P^* is the pressure of the hard cylinder system and v_0 is the volume of a cylinder. The average work function W is expanded as

$$\begin{aligned} W &= \sum_{i=1}^{m} S_i W_i(\alpha,\lambda) \\ &= C_{00} + C_{10}\alpha + C_{01}\lambda + C_{11}\alpha\lambda + C_{20}\alpha^2 + v_0 P^*\alpha^2\lambda \end{aligned} \tag{5}$$

where

$$C_{ab} = \frac{1}{a!b!}\left[\frac{\partial^{(a+b)}W}{\partial\alpha^a\partial\lambda^b}\right]_{\alpha=\lambda=0}$$

Using Eqs. (2–5), we get

$$C_{00}/kT = -\ln(1-d)$$

$$C_{10}/kT = d[2R\langle\sin\theta_{ij}\rangle + 4\langle E(\theta_{ij})\rangle/\pi]/(1-d)$$

$$C_{01}/kT = d[\langle|\cos\theta_{ij}|\rangle + 2\langle\sin\theta_{ij}\rangle/\pi R]/(1-d)$$

$$\begin{aligned} C_{11}/kT &= d[2\langle\sin\theta_{ij}\rangle/\pi R + \langle E(\theta_{ij})\rangle/\pi]/(1-d) + d^2[2R\langle\sin\theta_{ij}\rangle \\ &\quad + 4\langle E(\theta_{ij})\rangle/\pi] \times [\langle|\cos\theta_{ij}|\rangle + 2\langle\sin\theta_{ij}\rangle/\pi R]/(1-d)^2 \end{aligned}$$

$$C_{20}/kT = d[<|\cos\theta_{ij}|> + 2R<\sin\theta_{ij}>]/(1-d) + d^2[2R<\sin\theta_{ij}> + 4<E(\theta_{ij})>/\pi]^2/2(1-d)^2$$

where $R = r/l$, $d = v_0\rho$, and

$$E(\theta_{ij}) = \int_0^{\pi/2}\sqrt{1-\sin^2\theta_{ij}\sin^2\varphi}\,d\varphi$$

and

$$<x_{ij}> = \sum_{i=1}^{m}\sum_{j=1}^{m} S_i S_j x_{ij}.$$

By changing over to a continuous distribution of Ω_i and Ω_j, we can write

$$<x_{ij}> = \int_0^1 d\Omega_i \int_0^1 d\Omega_j f(\Omega_i)f(\Omega_j)x_{ij},$$

where $f(\Omega_i)$ and $f(\Omega_j)$ are the single particle distribution functions for the i^{th} and j^{th} type of cylinders. The average work function is now given by

$$W/kT = -\ln(1-d) + Ad/(1-d) + Bd^2/(1-d)^2 + v_0P^*/kT \quad (6)$$

where

$$A = (4R + 4/\pi R)<\sin\theta_{ij}> + 8<E(\theta_{ij})>/\pi + 2<|\cos\theta_{ij}|>$$

$$B = [R<\sin\theta_{ij}> + 2<E(\theta_{ij})>/\pi + <|\cos\theta_{ij}|> + 2<\sin\theta_{ij}>/\pi R] \times [2R<\sin\theta_{ij}> + 4<E(\theta_{ij})>/\pi].$$

In order to be able to develop the mean field theory, we expand $\sin\theta_{ij}$, $|\cos\theta_{ij}|$ and $E(\theta_{ij})$ in terms of even Legendre polynomials $[P_{2n}(\cos\theta_{ij})]$ and we get

$$\begin{aligned}<\sin\theta_{ij}> &= \frac{\pi}{4} - \frac{5\pi}{32}<P_2>^2 - \left(\frac{3}{16}\right)^2\pi<P_4>^2 - \frac{65}{(16)^3}\pi<P_6>^2 - -\\ <|\cos\theta_{ij}|> &= \frac{1}{2} + \frac{5}{8}<P_2>^2 - \left(\frac{3}{16}\right)<P_4>^2 + \frac{13}{16\times 8}<P_6>^2 - +\\ <E(\theta_{ij})> &= \frac{\pi^2}{8} + \frac{5\pi^2}{128}<P_2>^2 - \left(\frac{3}{16}\right)^3\pi^2<P_4>^2 + \frac{13}{2}\left(\frac{5\pi}{256}\right)^2<P_6>^2 - +\end{aligned} \quad (7)$$

where

$$<P_{2n}> = \int_0^1 P_{2n}(\Omega)f(\Omega)d\Omega \quad (8)$$

Substituting for $<\sin\theta_{ij}>$, $<|\cos\theta_{ij}|>$ and $<E(\theta_{ij})>$, A and B are simplified to

$$A = A_{000} + A_{200}<P_2>^2 + A_{020}<P_4>^2 + A_{002}<P_6>^2$$

$$\begin{aligned}B = B_{000} &+ B_{200}<P_2>^2 + B_{020}<P_4>^2 + B_{002}<P_6>^2 + B_{220}<P_2>^2<P_4>^2 \\ &+ B_{022}<P_4>^2<P_6>^2 + B_{202}<P_6>^2<P_2>^2 + B_{400}<P_2>^4 + B_{040}<P_4>^4 \\ &+ B_{004}<P_6>^4\end{aligned}$$

where

$$A_{000} = (R+1)(\pi R+1)/R$$

$$A_{200} = 5(1-2R)(\pi R-2)/16R$$

$$A_{020} = -4(3+9\pi R/8)(3+8R)/(16)^2R$$

$$A_{002} = 52(16R-5)(16-5\pi R)/(16)^4R$$

$$B_{000} = 2\pi(\pi R+2)(R+1)^2/16R$$

$$B_{200} = 20\pi(2R^2+R-1)(1-\pi R)/(16)^2R$$

$$B_{020} = 6\pi[\pi R(-24R^2-33R-9)+(-88R^2-121R-33)]/(16)^3R$$

$$B_{002} = 13\pi(11-5\pi R)(16R^2+11R-5)/(16)^4R$$

$$B_{220} = 30\pi(16R^2-2R-3)(3\pi R+2)/(16)^4R$$

$$B_{022} = 156\pi(256R^2+16R-30)(15\pi R-8)/(16)^7R$$

$$B_{202} = 520\pi(32R^2-26R+5)(5\pi R-26)/(16)^6R$$

$$B_{400} = 50\pi(2R-1)^2(\pi R-4)/(16)^3R$$

$$B_{040} = 216\pi(3\pi R+16)(8R+3)^2/(16)^6R$$

$$B_{004} = 1690\pi(256R^2-160R+25)(5\pi R-32)/(16)^8R.$$

The pressure for the hard particle system is obtained from the Gibbs-Duhem equation, viz.,

$$\left[\frac{\partial P^*/kT}{\partial\rho}\right]_{f(\Omega)} = 1 + d\left[\frac{\partial W/kT}{\partial d}\right]_{f(\Omega)} \qquad (9)$$

The above equation is solved with the relation (6), to get

$$P^*v_0/kT = d/(1-d) + Ad^2/2(1-d)^2 + 2Bd^3/3(1-d)^3 \qquad (10)$$

Equations (1), (6) and (10) can be combined to give the chemical potential μ^*,

$$\mu^* = \int \mu_i^* f(\Omega_i) d\Omega_i = \langle \ln f(\Omega_i) \rangle + \ln\left[\frac{\rho}{1-d}\right] + \frac{d}{1-d} + \frac{Ad(2-d)}{2(1-d)^2} + \frac{Bd^2(3-d)}{3(1-d)^3}, \quad (11)$$

hence the Helmholtz free energy of the hard cylinder system is

$$A_c^*/NkT = \mu^*/kT - P^* v_0/dkT = \langle \ln f(\Omega_i) \rangle - 1 + \ln[\rho/(1-d)] + Ad/2(1-d) + Bd^2/3(1-d)^2 \quad (12)$$

The normalized single particle distribution function $f(\Omega)$ which minimizes the Helmholtz free energy is given by

$$f(\Omega) = \frac{\mathrm{Exp}[-U_2(d)\langle P_2 \rangle P_2(\Omega) - U_4(d)\langle P_4 \rangle P_4(\Omega) - U_6(d)\langle P_6 \rangle P_6(\Omega)]}{\int_0^1 \mathrm{Exp}[-U_2(d)\langle P_2 \rangle P_2(\Omega) - U_4(d)\langle P_4 \rangle P_4(\Omega) - U_6(d)\langle P_6 \rangle P_6(\Omega)] d\Omega} \quad (13)$$

where

$$U_2(d) = \frac{dA_{200}}{1-d} + \frac{2d^2}{3(1-d)^2}[B_{200} + B_{220}\langle P_4 \rangle^2 + B_{202}\langle P_6 \rangle^2 + 2B_{400}\langle P_2 \rangle^2]$$

$$U_4(d) = \frac{dA_{020}}{1-d} + \frac{2d^2}{3(1-d)^2}[B_{020} + B_{220}\langle P_2 \rangle^2 + B_{022}\langle P_6 \rangle^2 + 2B_{040}\langle P_4 \rangle^2]$$

$$U_6(d) = \frac{dA_{002}}{1-d} + \frac{2d^2}{3(1-d)^2}[B_{002} + B_{202}\langle P_2 \rangle^2 + B_{022}\langle P_4 \rangle^2 + 2B_{004}\langle P_6 \rangle^2] \quad (14)$$

For the sake of completeness we give the expressions for the entropy change $\Delta S/Nk$ and the isothermal compressibility β of the isotropic phase:

$$\frac{\Delta S}{Nk} = \left(\frac{Pv_0}{kT}\right) \frac{d_{\mathrm{nem}} - d_{\mathrm{iso}}}{d_{\mathrm{nem}} d_{\mathrm{iso}}} \quad (15)$$

$$\beta = -\frac{1}{V}\left[\frac{\partial V}{\partial P}\right]_T = \frac{v_0}{dkT}\left[\frac{\partial(Pv_0/kT)}{\partial d}\right]_T$$

$$= \frac{v_0}{dkT}\left[\frac{1}{(1-d_{\rm iso})^2} + \frac{A_{000}d_{\rm iso}}{(1-d_{\rm iso})^3} + \frac{2B_{000}d_{\rm iso}^2}{(1-d_{\rm iso})^4}\right]^{-1} \quad (16)$$

RESULTS AND DISCUSSION

The properties of the ensemble are completely determined by the shape factor R and the packing fraction d. In Eq. 7, sin θ, $|\cos\theta|$ and $E(\theta)$ have been expanded in terms of even Legendre polynomials. It is necessary to truncate the series in order to make calculations. We have plotted the three functions of θ, by retaining terms up to the second, third and fourth terms in Figures 1a–1c. It is clear from the figures that the errors are reduced by including higher order terms. Retaining terms up to $P_6(\cos\theta)$ only, the error in $E(\theta)$ is quite small over the entire range of values of θ (Figure 1c), while the error for sin θ still remains noticeable for low angles (Figure 1b). Hence the usual approximation

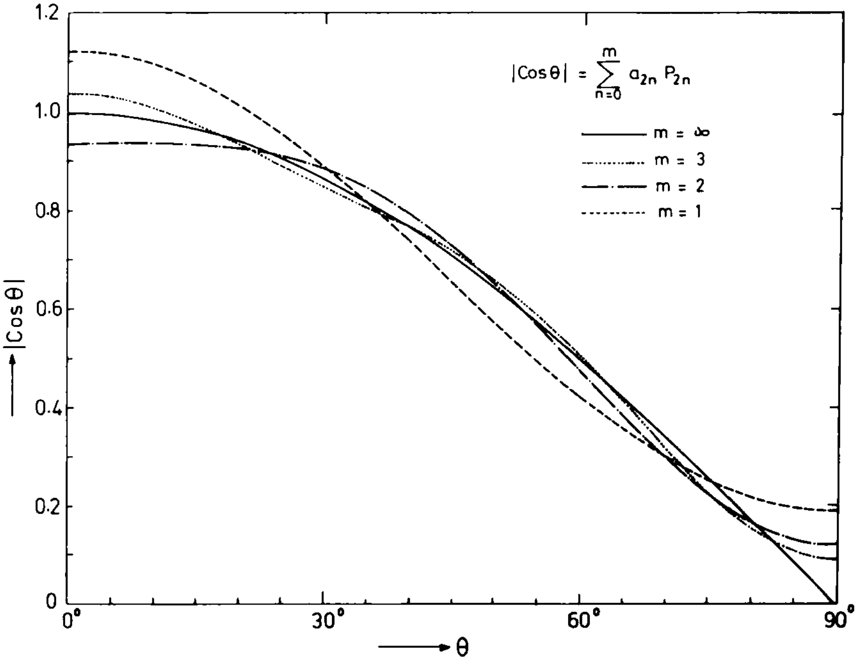

FIGURE 1a Comparison between $|\cos\theta|$ and the values obtained by retaining terms up to different even Legendre polynomials in the expansion given by Eq. (7).

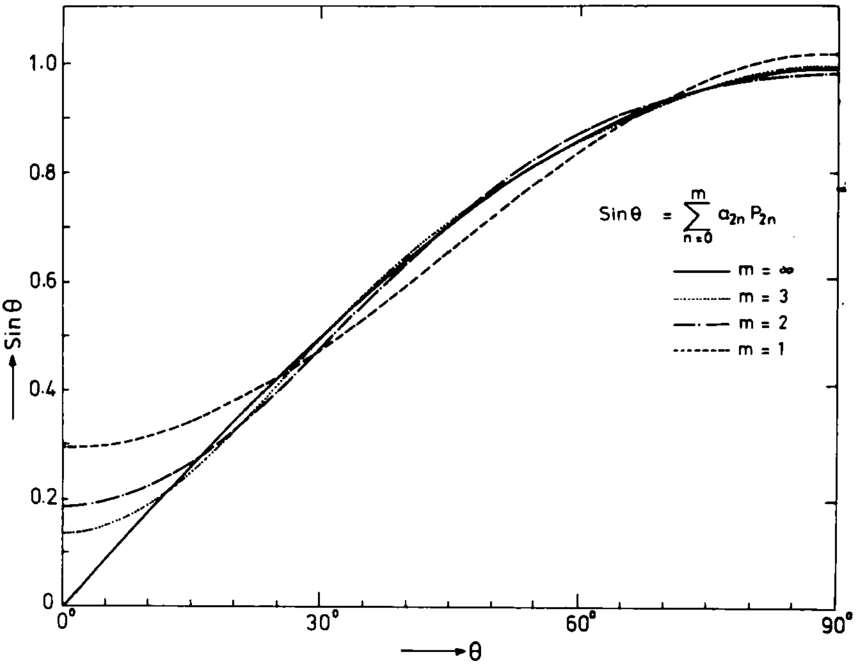

FIGURE 1b Comparison between sin θ and the values obtained by retaining terms up to different even Legendre polynomials in the expansion given by Eq. (7).

of retaining only the first two terms in the Eq. (7)[5,8,13] is likely to introduce considerable errors in the calculations. In fact in the present case, we shall see that the $P_4(\cos\theta)$ term is essential to get a qualitatively correct trend in the results. We have made calculations by retaining terms up to $P_2(\cos\theta)$, $P_4(\cos\theta)$ and $P_6(\cos\theta)$ respectively in the expansions (7) and correspondingly retaining terms up to $U_2(d)$, $U_4(d)$ and $U_6(d)$ respectively in Eq. (14).

For a given value of R, the calculations are made as follows. Assuming some reasonable value of d_{nem}, we can use Eq. (8) along with Eqs. (13) and (14) to get consistent values of $\langle P_{2n}\rangle$. The integrals have been evaluated on a DEC 10 computer by using a 16-points Gaussian quadrature scheme and the consistent values of $\langle P_{2n}\rangle$ have been obtained by adopting a least squares fitting procedure. The pressure can then be calculated using Eq. (10). Setting $\langle P_{2n}\rangle = 0$, the same equation can then be used to calculate the packing fraction of the isotropic phase (d_{iso}) by equating the pressure to that of the nematic phase. Equation (11) can now be used to calculate the chemical potentials of the two

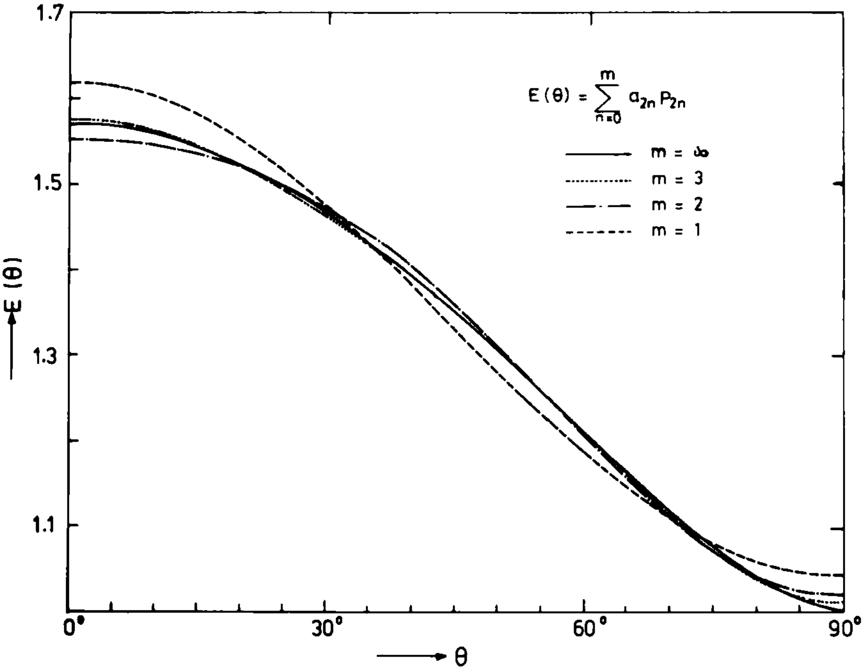

FIGURE 1c Comparison between $E(\theta)$ and the values obtained by retaining terms up to different even Legendre polynomials in the expansion given by Eq. (7).

phases. d_{nem} is now adjusted by an iterative procedure to make the chemical potentials of two phases equal. The calculations are repeated for a range of values of R between $R = 0.08$ (rod-like molecules) and $R = 3.0$ (disc-like molecules). The data are used to calculate $\Delta\rho/\bar{\rho}$ (which is the relative density change at N—I transition, $\bar{\rho} = (\rho_{\text{nem}} + \rho_{\text{iso}})/2$), the isothermal compressibility β of the isotropic phase and the entropy change at N—I transition. Retaining, in the first instance, only the first two terms in Eq. (7) the calculated values of $\langle P_2 \rangle$, d_{nem} and $\Delta\rho/\bar{\rho}$ at the N—I transition point as functions of R are shown in Figure 2. We see that the "rod-like" region ($R < 0.5$) gets very much compressed in the figure compared to the "disc-like" region ($R > 0.5$). Hence for a better comparison between the two regions, we have plotted the properties as functions of $2R$ for $R > 0.5$ and $1/2R$ for $R < 0.5$ in Figure 3. Figures 3a-3c correspond to calculations made by retaining terms up to $P_2(\cos\theta)$, $P_4(\cos\theta)$ and $P_6(\cos\theta)$ respectively as described above. The entropy change $\Delta S/Nk$ (Eq. 15), Pv_0/kT and the isothermal compressibility β (Eq. 16) of the isotropic phase at the N—I transition point are shown in Figures 4a-4c.

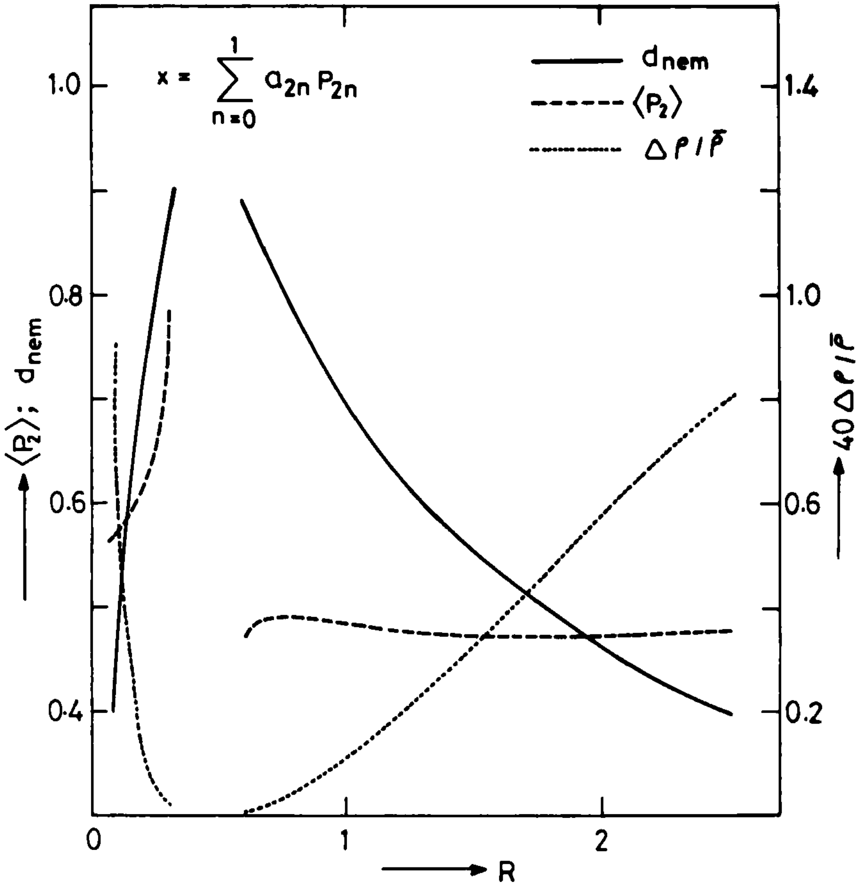

FIGURE 2 Variation of $<P_2>$, $d_{\rm nem}$ and $\Delta\rho/\bar{\rho}$ as functions of R obtained by retaining terms up to $P_2(\cos\theta)$ in Eq. (7).

When the expansion is restricted to terms up to $P_2(\cos\theta)$, it is seen from Eq. (14) and from the definition of A and B that there is no anisotropic phase for $R = 0.5$ (as was noticed by Isihara[13]). But by including higher order terms, we get the anisotropic phase for the entire range of values of R. Though $U_2(d) = 0$ for $R = 0.5$, $U_4(d)$ and $U_6(d)$ still contribute to the stability of the nematic phase. From Figure 3a, it is seen that as the shape anisotropy decreases, i.e., as the value of R approaches 0.5 from either side, $d_{\rm nem}$ at the N—I transition increases monotonically. However, the closest packed density for a system of right circular cylinders is $\pi/2\sqrt{3} \simeq 0.91$. We have not shown the results for the range $0.31 < R < 0.6$ in Figure 3a, since the calculated values of $d_{\rm nem}$ ex-

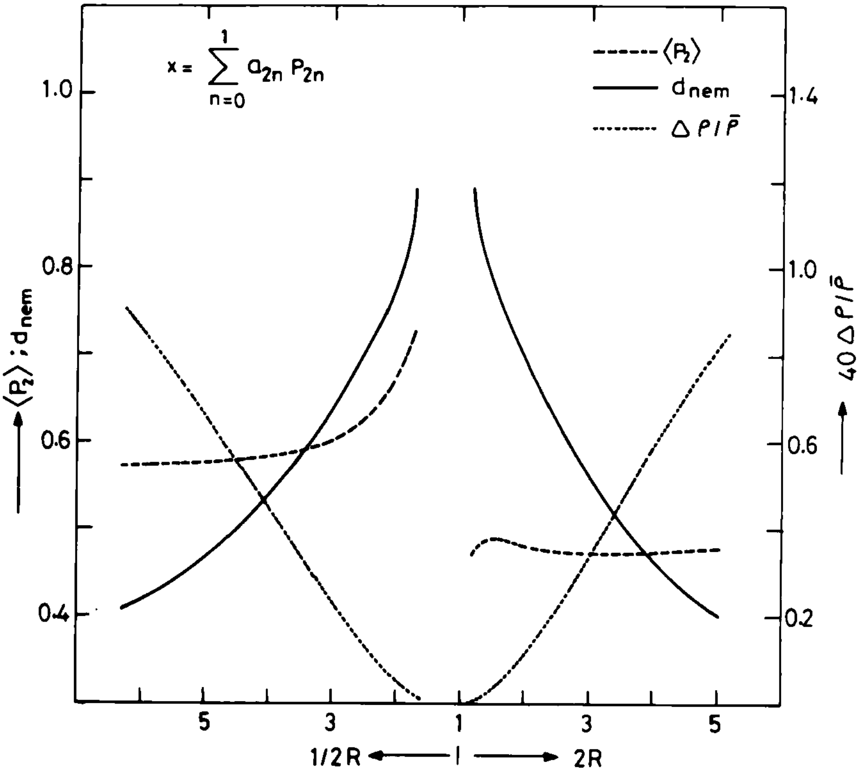

FIGURE 3a Variation of $<P_2>$, d_{nem} and $\Delta\rho/\bar{\rho}$ obtained by retaining terms up to $P_2(\cos\theta)$ in Eq. (7) and plotted as functions of $2R$ (for $R > 0.5$) and $1/2R$ (for $R < 0.5$).

ceed 0.91 in this range. This unphysical result is removed by including the higher order terms as is seen in Figures 3b and 3c, and d_{nem} at N—I point is a maximum for $R \simeq 0.47$. It means that less anisotropic particles exhibit the nematic phase at greater packing fractions. The density change $\Delta\rho/\bar{\rho}$ at the N—I transition decreases relatively rapidly as the anisotropy of the molecule is decreased. Retaining terms only up to $P_2(\cos\theta)$ in the expansion, $\Delta\rho/\bar{\rho}$ approaches zero. Including terms up to $P_4(\cos\theta)$ (Figure 3b) and $P_6(\cos\theta)$ (Figure 3c), $\Delta\rho/\bar{\rho}$ attains a minimum value $\simeq 0.008$ at $R \simeq 0.47$. Retaining terms only up to $P_2(\cos\theta)$, we found that $<P_2>$ decreases as the shape-anisotropy increases for the "rod-like" region. This trend is opposite to that for hard-spherocylinders.[8] On the other hand in the "disc-like" region the value of $<P_2>$ at N—I transition appears to be essentially independent of R (Figure 3a). However, this is an artifact of the approximation, since inclusion of higher order terms lead to a symmetric trend in the two sides (Figures 3b, 3c).

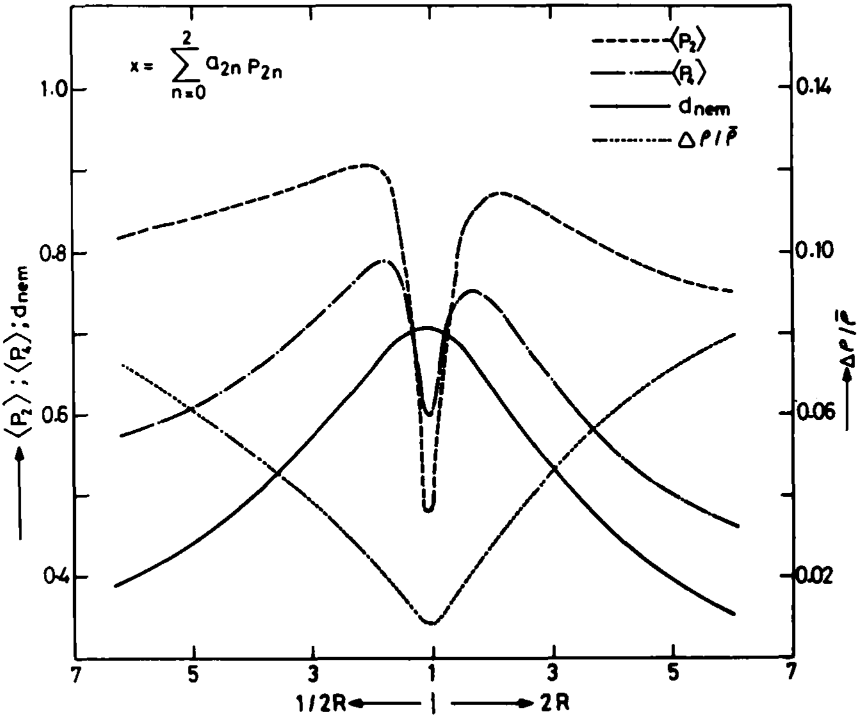

FIGURE 3b Variation of $<P_2>$, $<P_4>$, d_{nem} and $\Delta\rho/\bar{\rho}$ obtained by retaining terms up to $P_4(\cos\theta)$ in Eq. (7).

$<P_{2n}>$ increases as the anisotropy decreases, attains a maximum and has a sharp dip as we approach $R = 0.5$ taking a minimum value for $R \simeq 0.47$. As seen in the same figures, $<P_4>$ has higher values than $<P_2>$ in a small range of values of $2R$ around $2R = 1$. The maximum value of $<P_{2n}>$ in the "rod-like" region is somewhat larger than that in the "disc-like" region. From Figures 3a–3c, selecting the value of R such that $(2R)_{\text{disc-like}} = (1/2R)_{\text{rod-like}}$, we found that $<P_{2n}>$, d_{nem} and $\Delta\rho/\bar{\rho}$ for rod-like molecules are somewhat larger than those of the disc-like molecules. Further the product of $(2R)_{\text{disc-like}} \times (1/2R)_{\text{rod-like}}$ for cylinders having the same value of d_{nem} at the N—I transition is seen to be $\simeq 0.8$.

The trends in other properties of the nematic phase are also changed somewhat as a consequence of introducing higher order terms. The entropy change $\Delta S/Nk$ at N—I transition point increases as the shape anisotropy decreases, attains a maximum and decreases sharply attaining a minimum value $\simeq 0.98$ for $R \simeq 0.47$ (Figures 4b and 4c). Experimentally it has been found that $\Delta S/Nk$

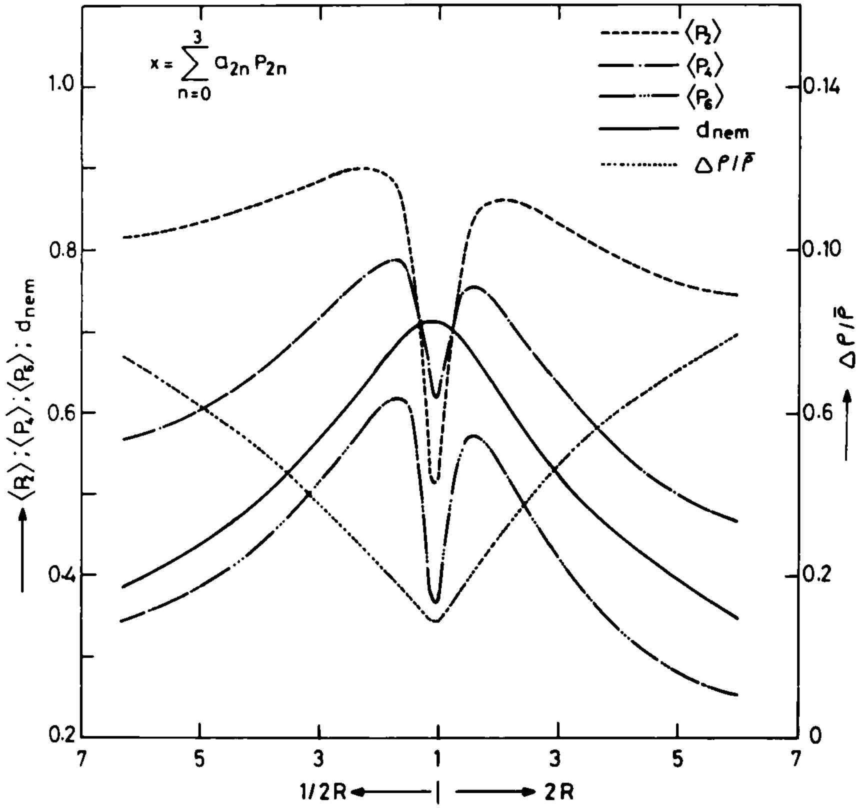

FIGURE 3c Variation of $<P_2>$, $<P_4>$, $<P_6>$, d_{nem} and $\Delta\rho/\bar{\rho}$ obtained by retaining terms up to $P_6(\cos\theta)$ in Eq. (7).

$\sim 0.06^{14}$ for $R \simeq 9$. The calculated value is an order of magnitude larger. The purely hard rod model[5,8] which leads to relatively larger values for $<P_{2n}>$ and $\Delta\rho/\bar{\rho}$, also causes the large entropy change. This may be improved by taking the intermolecular attractive forces into account. Pv_0/kT increases as R approaches 0.5 from either side and reaches a maximum $\simeq 80$ for $R \simeq 0.47$. Assuming that the pressure is held constant, N—I transition temperature increases as the anisotropy increases. This trend agrees with the experimental results for the rod-like molecules. On the other hand, the experimental data[14] on disc-like molecules seems to give the opposite trend. Further the isothermal compressibility β of the isotropic phase decreases as R decreases to 0.5 from either side and attains a minimum $\simeq 0.1 \times 10^{-10}$ cm^2/dyne at $R \simeq 0.47$.

In conclusion, we can see that it is necessary to introduce higher order terms, at least up to $P_4(\cos\theta)$ in the expansions, to get qualitatively correct

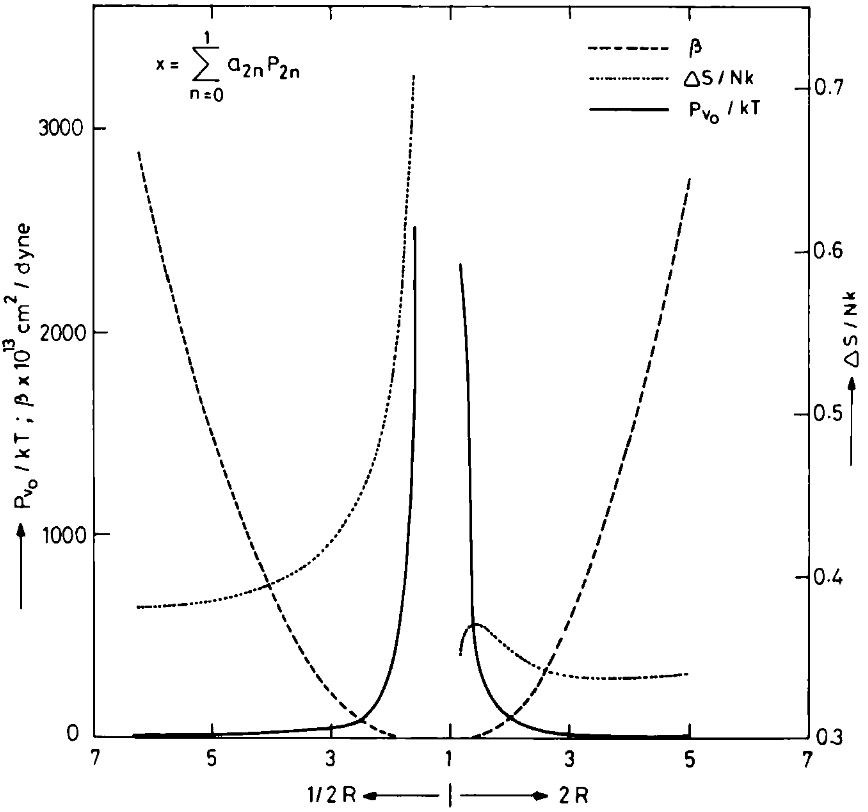

FIGURE 4a $\Delta S/Nk$, Pv_0/kT and β obtained by retaining terms up to $P_2(\cos\theta)$ in Eq. (7).

results. Including the next higher order term, viz., $P_6(\cos\theta)$, the qualitative behavior of the properties of the nematic-isotropic transition remain practically the same, but there are minor quantitative changes. Hence the addition of further terms of the expansion is not necessary for studying the behavior of N—I transition of "rod-like" and "disc-like" molecules.

We are now making calculations by including an attractive potential also. The results will be discussed elsewhere.

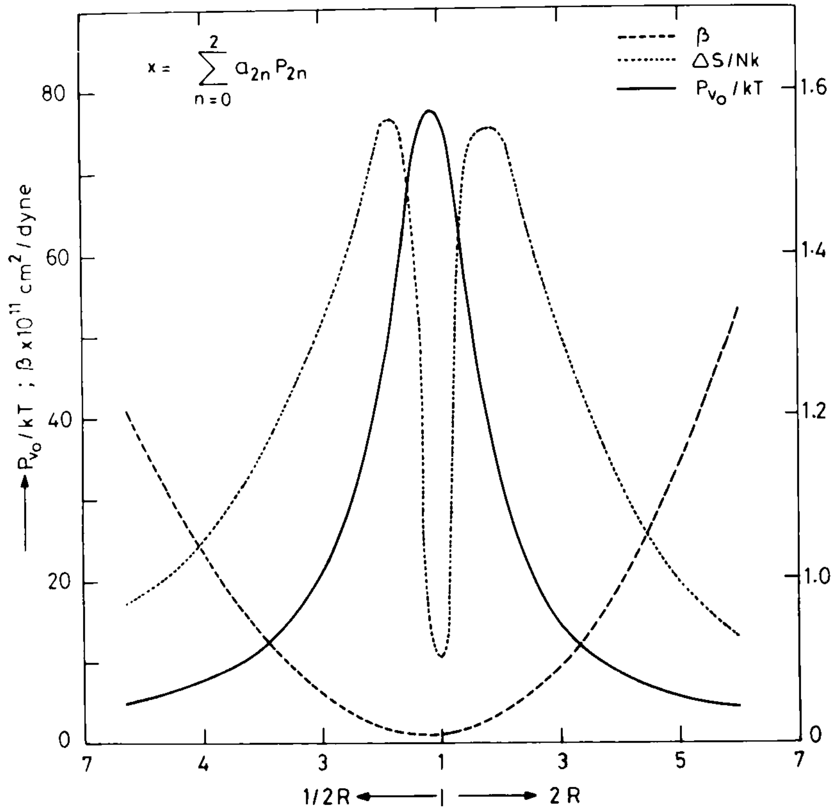

FIGURE 4b $\Delta S/Nk$, Pv_0/kT and β obtained by retaining terms up to $P_4(\cos\theta)$ in Eq. (7).

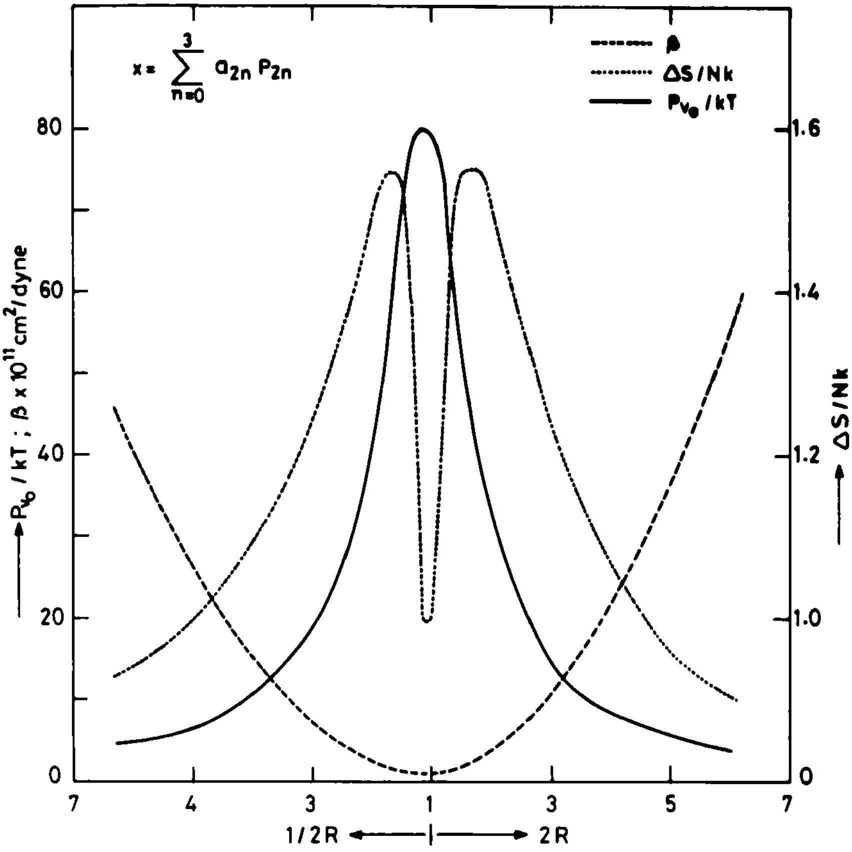

FIGURE 4c $\Delta S/Nk$, Pv_0/kT and β obtained by retaining terms up to $P_6(\cos\theta)$ in Eq. (7).

Acknowledgment

We are indebted to Prof. S. Chandrasekhar for some useful discussions.

References

1. L. Onsager, *Phys. Rev.*, **62,** 558 (1942); *Ann. N.Y. Acad. Sci.*, **51,** 627 (1949).
2. R. Zwanzig, *J. Chem. Phys.*, **39,** 1714 (1963).
3. R. Alben, *Mol. Cryst. Liq. Cryst.*, **13,** 193 (1971).
4. M. A. Cotter and D. E. Martire, *Mol. Cryst. Liq. Cryst.*, **7,** 295 (1969); *J. Chem. Phys.*, **52,** 1909 (1970).
5. M. A. Cotter, *J. Chem. Phys.*, **66,** 1098 (1977).
6. J. G. J. Ypma and G. Vertogen, *Phys. Lett.*, **61A,** 125 (1977).
7. B. A. Baron and W. M. Gelbart, *J. Chem. Phys.*, **67(12),** 5795 (1977).
8. K. L. Savithramma and N. V. Madhusudana, *Mol. Cryst. Liq. Cryst.*, **62,** 63 (1980).
9. S. Chandrasekhar, B. K. Sadashiva and K. A. Suresh, *Pramana*, **9(5),** 471 (1977).
10. N. H. Tinh, C. Destrade and H. Gasparoux, *Phys. Letters*, **72A,** 251 (1979).
11. J. D. Brooks and G. H. Taylor, *Carbon*, **3,** 185 (1965).
12. R. Alben, *Phys. Rev. Lett.*, **30,** 778 (1973).
13. A. Isihara, *J. Chem. Phys.*, **19,** 1142 (1951).
14. C. Destrade, M. C. Bernaud, H. Gasparoux, A. M. Levelut and Nguyen Huu Tinh, in Liquid Crystals, Proceedings of the International Liquid Crystals Conference, Bangalore, 1979, Ed. S. Chandrasekhar, Heyden, London, p. 29.